

Analysis of reverse-bias leakage current mechanisms in GaN grown by molecular-beam epitaxy

E. J. Miller and E. T. Yu^{a)}

Department of Electrical and Computer Engineering, University of California, San Diego, La Jolla, California 92093-0407

P. Waltereit and J. S. Speck

Materials Department University of California, Santa Barbara, Santa Barbara, California 93106

(Received 6 October 2003; accepted 26 November 2003)

Temperature-dependent current–voltage measurements have been used to determine the reverse-bias leakage current mechanisms in Schottky diodes fabricated on GaN grown by molecular-beam epitaxy, and two dominant mechanisms are clearly identified. The first mechanism is field-emission tunneling from the metal into the semiconductor, which is dominant at low temperatures and which, at higher temperatures, becomes significant for large reverse-bias voltages. The second mechanism, presumed to be associated with dislocation-related leakage current paths, is observed to have an exponential temperature dependence and becomes significant above approximately 275 K. The temperature dependence of the second mechanism is consistent with either one-dimensional variable-range-hopping conduction along the dislocation or trap-assisted tunneling. © 2004 American Institute of Physics. [DOI: 10.1063/1.1644029]

Reverse-bias Schottky diode leakage presents a major technological drawback to using GaN grown by molecular-beam epitaxy (MBE) in both vertical and lateral current flow electronic devices. Leakage has been studied extensively in MBE-grown GaN, and a number of solutions to decrease the leakage current have recently been proposed.^{1–4} Current paths associated with threading dislocations (TDs), which occur in high concentrations in MBE-grown GaN, have been shown to be the dominant source of LC at room temperature.^{5–7} These are typically observed using conductive atomic force microscopy (AFM), in which one applies a voltage between the AFM tip and the sample, and measures conductivity variations across the sample by recording the localized current flow. Conductive AFM has therefore been extremely useful in identifying TDs as the primary source of leakage current at room temperature, but it does not provide information about the exact mechanism of current flow associated with the dislocations.

Temperature-dependent current–voltage measurements of Schottky diodes fabricated on MBE-grown GaN provide a method to investigate the physical mechanisms associated with the reverse-bias leakage current in the material. To evaluate the plausibility of various conduction mechanisms, the measured currents can be compared to the current levels that would be predicted by these conduction models for different temperatures and voltages to ensure the models describe the entire data set. Using this method, the present investigation reveals the presence of two distinct leakage current mechanisms: one associated with field-emission tunneling and another with an exponential temperature dependence consistent with either trap-assisted tunneling or one-dimensional hopping conduction presumed to be associated with the TDs in the material.

GaN samples were grown by MBE on a template that consisted of a 2 μm GaN layer grown by metalorganic chemical vapor deposition on a sapphire substrate. A 350 nm MBE GaN layer was grown at 660 °C close to the upper crossover point in the Ga droplet regime⁸ with a dopant concentration in the mid- 10^{16} cm^{-3} range. Schottky diodes were fabricated on the surface of the sample using Ti/Al/Ti/Au metallization⁹ annealed at 750 °C for 30 s for the ring-shaped ohmic contacts with circular Ni Schottky contacts 125 μm in diameter in the centers of the ohmic contacts.

To determine the mechanisms responsible for the observed leakage current, various current transport models were compared to the measured data; each of the possible mechanisms is illustrated schematically in Fig. 1. Considering the Schottky barrier height, discussed later, thermionic emission over the barrier should have been negligibly small compared to the measured current levels, and it will therefore be neglected in the following discussion. Current–voltage measurements were performed for temperatures from 125 to 400 K and reverse bias voltages up to -20 V. Figure 2 shows

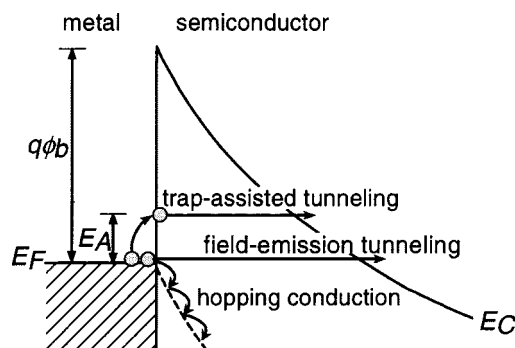


FIG. 1. Schematic diagram showing possible conduction mechanisms responsible for RBLC in MBE-grown Schottky diodes.

^{a)}Electronic mail: ety@ece.ucsd.edu

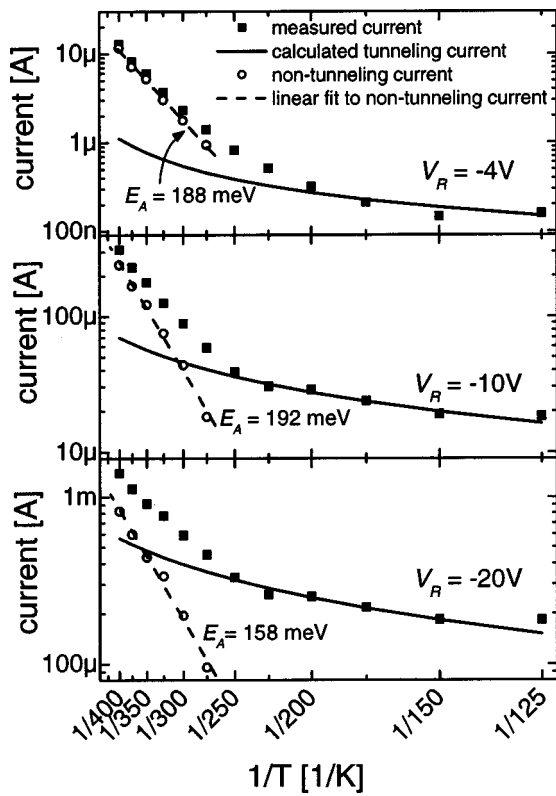


FIG. 2. Measured current–temperature characteristics for a Schottky diode at three different RB voltages (squares); calculated tunneling currents, which describe the data well in the lower temperature regime (solid lines); the nontunneling current component (circles); and straight-line fits to the non-tunneling current (dashed lines), suggesting a thermally activated mechanism with an activation energy of approximately 180 ± 20 meV.

an Arrhenius plot of the current in a typical Schottky diode for three voltages.

At low temperatures, the dominant mechanism for current transport is found to be field-emission tunneling. In this model, the current flow due to tunneling of electrons from the metal into the semiconductor is given by¹⁰

$$J_{m \rightarrow s} = \frac{A^* T}{k} \int_0^{qV_b} F_m T(\eta) (1 - F_s) d\eta, \quad (1)$$

where A^* is the effective Richardson’s constant, T is the absolute temperature, k is Boltzmann’s constant, F_m and F_s are the Fermi–Dirac distribution functions in the metal and semiconductor, qV_b is the difference in energy between the top of the Schottky barrier and the conduction band of the undepleted semiconductor, η is the energy below the top of the Schottky barrier, and $T(\eta)$ is the quantum transmission coefficient of the electrons through the approximately triangular Schottky barrier, given by

$$T(\eta) = \exp\left(-\frac{\eta^{3/2}}{\sqrt{qV_b}} \frac{8}{3} \sqrt{\frac{m^* \epsilon_s}{N_D}} \frac{1}{q\hbar}\right), \quad (2)$$

where m^* is the semiconductor electron effective mass, N_D is the donor concentration, q is the electron charge, ϵ_s is the semiconductor dielectric constant, and \hbar is the reduced Planck’s constant. Under reverse bias, the states in the conduction band can be taken as unoccupied, yielding $(1 - F_s) \approx 1$.

The relevant parameters used in fitting the tunneling-current model to the measured data are A^* , ϕ_b , and the ratio of N_D to the relative effective mass, $\beta \equiv N_D / (m^* / m_0)$. A^* and ϕ_b were extracted³ from forward-bias I – V measurements taken at several temperatures using the Norde method,¹¹ which yielded values of 0.0010 ± 0.0004 A/cm² K² and 0.798 ± 0.014 V, respectively. This value for ϕ_b agrees well with other values reported for Schottky contacts to n -GaN.^{12–14} The value for A^* is significantly lower than the theoretically predicted value of 26 A/cm² K²,¹⁵ but comparable to other reported values for the effective Richardson constants of GaN Schottky diodes.¹⁶ The ratio of the donor concentration to the relative effective mass is therefore the only fitting parameter in the model.

The tunneling-current model was found to fit the measured data for different voltages for temperatures of 125 K to approximately 250 K. The ratio β needed to fit the data in this temperature regime was approximately 5.1×10^{19} cm^{–3}, and the tunneling currents calculated using this value are shown by the solid lines in Fig. 2. This value of β can be achieved using reasonable values for the doping concentration and the relative effective mass. With a doping concentration of 5×10^{16} cm^{–3}, a relative effective mass of 9.8×10^{-3} gives the correct ratio β to fit the measured data to the tunneling-current model in the low-temperature regime. The effective Richardson constant based on this value of the effective mass agrees with other reported values of A^* for n -GaN Schottky diodes, which tend to vary over a wide range.¹⁶ The discrepancy between the effective mass predicted by this analysis and that measured elsewhere¹⁷ to be $0.222 m_0$ is most likely due to additional transport mechanisms such as defect-assisted tunneling, which increases the tunneling transmission probability. However, the general agreement between the tunneling currents, which were calculated using physically reasonable values for the model parameters, and the measured low-temperature data, suggests that tunneling current is, in fact, dominant in the low-temperature regime.

The calculated tunneling currents can then be subtracted from the measured data for each voltage, as shown in Fig. 2. The resulting data set, referred to as the “nontunneling” current herein, appears linear on the Arrhenius plot, suggesting a thermally activated mechanism with an $\exp(-E_A/kT)$ functional dependence, where E_A is an activation energy as discussed later. A linear fit to each data set yields $E_A = 180 \pm 20$ meV, which remains nearly constant for voltages ranging from -4 to -20 V. The consistency of E_A over such a large range of voltages is noteworthy as potential validation of the significance of this current mechanism at room temperature and above.

One possible physical mechanism associated with this thermally activated current component is a two-step, trap-assisted tunneling process. In such a model, an electron in the metal could be thermally activated to a trap state at the metal–semiconductor interface and then tunnel into the semiconductor, as shown in Fig. 1. Assuming thermal activation is the rate-limiting step, the trap state would then be at an energy $\phi_b - E_A = 0.62$ eV below the conduction band edge of the semiconductor. Given the experimental uncertainties

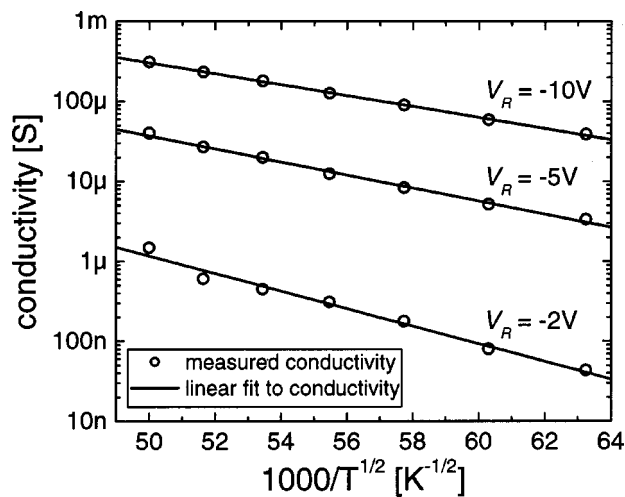


FIG. 3. Measured Schottky diode conductivity as a function of $1/T^{1/2}$ for selected RB bias voltages showing a linear dependence in the high-temperature regime, consistent with one-dimension VRH conduction along the threading dislocations in the semiconductor.

in E_A and ϕ_b , the uncertainty in the energy level of this trap state is estimated to be ± 0.03 eV.

Another possible current mechanism that could account for the thermally activated current is conduction from the metal into the semiconductor that occurs along the TDs. In this case, an electron in the metal would fall into a state associated with a TD very near or below the Fermi level in the metal with subsequent transport described by a one-dimensional variable-range-hopping (1D-VRH) conduction model. The conductivity would then be given by¹⁸

$$\sigma = \sigma_0 \exp[-(T_0/T)^{1/2}], \quad (3)$$

where T_0 is a characteristic temperature. Plotting the log of the measured conductivity of a Schottky diode as a function of $1/T^{1/2}$ yields a straight line for temperatures from 250 to 400 K, as shown in Fig. 3. It is therefore difficult to determine based on these data alone whether trap-assisted tunneling or 1D-VRH is the more likely conduction mechanism in this temperature regime, since both models appear consistent with the measured data.

Other studies of leakage current in MBE-grown GaN have shown it to be dominated by a conduction mechanism associated with the TDs in the material.^{5,6} Investigations of trap states in very similar MBE-grown GaN material have found energy levels at 0.59 and 0.91 eV below the conduction band edge.¹⁹ The activation energy and the capture cross section of the trap state at $E_C - 0.91$ eV were found to vary with the Ga/N flux ratio during growth, suggesting that the 0.91 eV level may be related to the nature of TDs which have been shown to display variations in conductivity for different growth conditions.²⁰ Further evidence that the 0.91 eV level is associated with TDs and could therefore be related to the current observed in this investigation is provided by the capture kinetics of the trap, which display the behavior of interacting point defects arranged along a line.²¹ Thus, it is very possible that the nontunneling current observed here is re-

lated to this energy level due to the mutual relation to TDs. On this basis, it appears that the 1D-VRH conduction model may be the more likely origin of the nontunneling current component.

In summary, an investigation of the reverse-bias leakage current mechanisms in Schottky diodes on *n*-type GaN grown by MBE has been performed. At lower temperatures, field-emission tunneling from the metal into the semiconductor was the dominant mechanism, and for large voltages, this tunneling current was significant over the entire range of measured temperatures. For temperatures of approximately 275 to 400 K, a thermally activated mechanism with an exponential temperature dependence was clearly identifiable. This mechanism was associated with either a two-step, trap-assisted tunneling process with an activation energy of approximately 180 meV or one-dimensional variable-range-hopping conduction along the threading dislocations in the material.

Part of this work was supported by ONR (POLARIS MURI, Grant No. N00014-99-1-0729 monitored by Dr. Colin Wood) and BMDO (monitored by Dr. Kepi Wu).

- ¹L. McCarthy, I. Smorchkova, H. Xing, P. Fini, S. Keller, J. Speck, S. P. DenBaars, M. J. W. Rodwell, and U. K. Mishra, *Appl. Phys. Lett.* **78**, 2235 (2001).
- ²M. A. Khan, X. Hu, A. Tarakji, G. Simin, J. Yang, R. Gaska, and M. S. Shur, *Appl. Phys. Lett.* **77**, 1339 (2000).
- ³E. J. Miller, D. M. Schaadt, E. T. Yu, P. Waltereit, C. Poblenz, and J. S. Speck, *Appl. Phys. Lett.* **82**, 1293 (2003).
- ⁴J. Spradlin, S. Dogan, M. Mikkelsen, D. Huang, L. He, D. Johnstone, H. Morkoç, and R. J. Molnar, *Appl. Phys. Lett.* **82**, 3556 (2003).
- ⁵J. W. P. Hsu, M. J. Manfra, D. V. Lang, S. Richter, S. N. G. Chu, A. M. Sergent, R. N. Kleiman, L. N. Pfeiffer, and R. J. Molnar, *Appl. Phys. Lett.* **78**, 1685 (2001).
- ⁶E. J. Miller, D. M. Schaadt, E. T. Yu, C. Poblenz, C. Elsass, and J. S. Speck, *J. Appl. Phys.* **91**, 9821 (2002).
- ⁷E. J. Miller, D. M. Schaadt, E. T. Yu, X. L. Sun, L. J. Brillson, P. Waltereit, and J. S. Speck, *J. Appl. Phys.* (in press).
- ⁸B. Heying, I. Smorchkova, C. Poblenz, C. Elsass, P. Fini, S. DenBaars, U. Mishra, and J. S. Speck, *Appl. Phys. Lett.* **77**, 2885 (2000).
- ⁹D. F. Wang, S. Feng, C. Lu, A. Motayed, M. Jah, S. N. Mohammad, K. A. Jones, and L. Salamanca-Riba, *J. Appl. Phys.* **89**, 6214 (2001).
- ¹⁰E. J. Miller, X. Z. Dang, and E. T. Yu, *J. Appl. Phys.* **88**, 5951 (2000).
- ¹¹T. Chot, *Phys. Status Solidi A* **66**, K43 (1981).
- ¹²J. D. Guo, F. M. Pan, M. S. Feng, R. J. Guo, P. F. Chou, and C. Y. Chang, *J. Appl. Phys.* **80**, 1623 (1996).
- ¹³A. C. Schmitz, A. T. Ping, M. Asif Khan, Q. Chen, J. W. Yang, and I. Adesida, *Semicond. Sci. Technol.* **11**, 1464 (1996).
- ¹⁴Q. Z. Liu, L. S. Yu, F. Deng, S. S. Lau, and J. M. Redwing, *J. Appl. Phys.* **84**, 881 (1998).
- ¹⁵M. Khan, T. Detchprohm, P. Hacke, K. Hiramatsu, and N. Sawaki, *J. Phys. D* **28**, 1169 (1995).
- ¹⁶L. S. Yu, Q. Z. Liu, Q. J. Xing, D. J. Qiao, and S. S. Lau, *J. Appl. Phys.* **84**, 2099 (1998).
- ¹⁷A. M. Witowski, K. Pakula, J. M. Baranowski, M. L. Sadowski, and P. Wyder, *Appl. Phys. Lett.* **75**, 4154 (1999).
- ¹⁸H. Iwano, S. Zaima, and Y. Yasuda, *J. Vac. Sci. Technol. B* **16**, 2551 (1998).
- ¹⁹A. Hierro, A. R. Arehart, B. Heying, M. Hansen, U. K. Mishra, S. P. DenBaars, J. S. Speck, and S. A. Ringel, *Appl. Phys. Lett.* **80**, 805 (2000).
- ²⁰J. W. P. Hsu, M. J. Manfra, S. N. G. Chu, C. H. Chen, L. N. Pfeiffer, and R. J. Molnar, *Appl. Phys. Lett.* **78**, 3980 (2001).
- ²¹A. Hierro, A. R. Arehart, B. Heying, M. Hansen, J. S. Speck, U. K. Mishra, S. P. DenBaars, and S. A. Ringel, *Phys. Status Solidi B* **228**, 309 (2001).